ELECTRON CLOUD STUDIES FOR HEAVY-ION AND PROTON MACHINES[*]

F. Petrov, O. Boine-Frankenheim, Th. Weiland
Computational Electromagnetics Laboratory, Technische Universität Darmstadt, Germany

Abstract

Electron cloud effects are a known problem in various accelerator facilities around the world. Electron clouds cause instabilities and emittance growth in positron and proton beams as well as in heavy ion beams. Most of the hadron machines experience the build-up of EC due to the multipacting. In LHC and in positron machines production of electrons due to the synchrotron radiation becomes as important as the build-up due to the secondary emission. The main source of seed electrons in heavy ion machines is the residual gas ionization. FAIR facility in Darmstadt will operate with heavy-ion and proton beams. However, the beam parameters are such that the multipacting will start to play a role only for the unconditioned wall with the secondary emission yield more than 1.8. In this paper we study the electron cloud build-up and its effect on the beam stability for FAIR heavy-ion coasting beams. These beams will be used during slow extraction. Electron scattering on the beam ions and its effect on the final neutralization degree and stability is discussed. In this contribution we also present simulation results for LHC and SPS like short proton bunches. We compare the electron cloud induced wake fields obtained using VORPAL and simplified code with 2D Poisson solver. The stopping powers obtained in the simulations are compared with the analytical theory.

INTRODUCTION

Electron clouds are dangerous for positively charged beams. Electron cloud effects have been observed worldwide [1]. They appear in the accelerators with short relativistic bunches and in machines with long coasting beam like bunches. The main source of the electron cloud build-up is usually the multipacting. Electrons accumulated from the preceding passages of the bunches are accelerated towards the wall by the field of the following bunches. In this case the accumulation of the cloud strongly depends on the wall properties. The studies concerning the theoretical and experimental investigation of the secondary electron production can be found in [2, 3]. It is known that the LHC suffers from the electron cloud build-up during the operation with 25 ns bunch spacings. In FAIR the build-up of electron cloud may happen for the secondary emission yields higher than 1.8 for the bunched beams [2, 4]. In case of coasting beams no multipacting is predicted. The only source of electrons left is residual gas ionization. This paper consists of two parts. In the first part we investigate the effect of the residual gas electrons on the stability of FAIR beams and

find the equivalence of different heavy-ion beams at certain conditions. In the second part we shortly describe the studies of electron cloud stopping powers and wake fields already published in [5]. Moreover we add a comparison of the transverse electron cloud wake fields simulated using different codes.

LINEAR THEORY OF TWO-STREAM INSTABILITY

Coupled equations of motion for positively charged beam and electron cloud can be written as follows [6]:

$$\left(\frac{\partial}{\partial t} + \omega_0 \frac{\partial}{\partial \theta}\right)^2 y_i + \omega_\beta^2 y_i = \omega_i^2(t)(y_i - \bar{y}_e) + \omega_{i,s}^2(y_i - \bar{y}_i)$$

$$\frac{d^2 y_e}{dt^2} = -\omega_e^2(y_e - \bar{y}_i) + \omega_{e,s}^2(t)(y_e - \bar{y}_e)$$

(1)

where $\omega_e = Q_e \omega_0$ - electron oscillation tune; $\omega_i = Q_i \omega_i$ - ion oscillation tune in the field of electrons in the absence of external focusing; $\omega_{i,s} = Q_{i,s}\omega_0$ and $\omega_{e,s} = Q_{e,s}\omega_0$ - perturbations of the tune by self-fields. For further studies we neglect the self-field terms. In this case Eq. 1 can be solved analytically for constant electron density to obtain the instability growth rate. Taking into account beam tune spread and electron frequency spread due to the nonlinear fields one obtains the stability condition [7, 8].

$$\frac{\Delta Q_\beta}{Q_\beta} \cdot \frac{\Delta Q_e}{Q_e} \gtrsim \frac{Q_i^2}{Q_\beta^2}$$

(2)

In reality the electrons are constantly produced. This leads to the variation of ω_i and $\omega_{e,s}$ in time. Most of the observations and theoretical works [9, 10] indicate that the ionization cross sections of residual gas by different ions scale as follows

$$\sigma_{ion} \propto Z^2$$

(3)

where Z - charge state of the beam ion. This means that the time in which the beam is neutralized in the absence of interaction with electron cloud is $\propto Z$.

Heavy ion synchrotron SIS100 will operate with a broad variety of heavy ions. These beams will have different intensities depending on their mass A and charge Z states. The main intensity limiting factor is space charge tune shift at 11.4 MeV/u [11]. There are also limiting factors depending on the ion source. However, further we assume that the total beam charge is limited only by the space charge tune

shift. This tune shift should be one and the same for all the species.

$$\Delta Q_y = -\frac{2N_i Z^2 g_f}{\pi A \beta_0^2 \gamma_0^3 B_f (\epsilon_y + \sqrt{\epsilon_y \epsilon_x})} \propto \frac{N_i Z^2}{A} \quad (4)$$

where B_f - bunching factor; $\epsilon_{x,y}$ - transverse emittances; N_i - number of beam particles; A - mass number; Z - charge state; β_0, γ_0 - relativistic parameters. This equation gives us the scaling for the beam intensity depending on the ion parameters

$$N_i \propto \frac{A}{Z^2} \quad (5)$$

Different beams will have one and the same transverse emittance due to the fixed acceptance at the injection energy. This means equal beam sizes. Electron trapping frequency in case of round Gaussian beam is given as follows

$$\omega_e = Q_e \omega_0 = \sqrt{\frac{Z N_i e^2}{4\pi\epsilon_0 m_e L \sigma_r^2}} \propto \sqrt{\frac{A}{Z}} \quad (6)$$

The instability harmonic n is proportional to the electron trapping frequency. The threshold instability growth rate in case of corrected chromaticity and negligible space charge effect is the following [12]:

$$\frac{1}{\tau_{inst}} = \sqrt{\frac{2}{\pi}} \Delta \omega_n = \sqrt{\frac{2}{\pi}} \omega_e \eta \frac{dp}{p} \propto \sqrt{\frac{A}{Z}} \quad (7)$$

On the right side of the Eq. 1 for ion motion one sees the driving term from electrons. This term is given by the equation

$$\omega_i = \omega_0 Q_i = \sqrt{\frac{Z n_e e^2}{4\pi\epsilon_0 A m_0 L \sigma_r^2 \gamma_0}} = \omega_0 Q_e \sqrt{\chi_e \frac{Z m_e}{\gamma_0 A m_0}} \quad (8)$$

where χ_e is the neutralization factor (total electron charge divided by the total beam charge). If electron cloud is produced due to the residual gas ionization at least 60% of all electrons are produce outside the rms radius of the beam. That is why the cloud is originally very nonlinear and has a significant spread.

Under the SIS100 conditions the ratio $\Delta Q_e / Q_e \approx const$ independent of specie's type. Substituting Eq. 8 into Eq. 2 one gets

$$\frac{\Delta Q_\beta}{Q_\beta} \cdot \frac{\Delta Q_e}{Q_e} \gtrsim \frac{Q_e^2}{Q_\beta^2} \chi_e \frac{Z m_e}{\gamma_0 A m_0} \quad (9)$$

Taking into account Eq. 6 one sees that the threshold neutralization degree for different ions at fixed energy does not depend on the species parameters.

There are different fits for the ionization cross sections of residual gas by beam ions. However, most of them show similar behaviour depending on the charge state of the ion. Ionization rate is directly proportional to the cross section

value. Hereafter, it is convenient to talk in terms of normalized ionization cross sections and ionization rates

$$\sigma_{ion,n} = \sigma_{ion}/Z \propto Z \quad (10)$$

The neutralization rate is given as follows

$$V_{neut} = \sigma_{ion,n} \beta_0 c \rho_g N_i \quad (11)$$

One sees immediately that heavy ion U^{73+} will reach the instability threshold 73 times faster than proton. In this sense the proton beam is equivalent to the heavy ion beam with charge state Z, if the proton beam is operated at Z times higher pressure.

HEATING RATE

In [13] the Coulomb heating was proposed as a mechanism leading to the loss of electrons trapped in the beam. Electrons continuously collide with the beam particles leading to the diffusion in the electron velocity space. In [13] the heating rate is obtained assuming that the beam is infinite transversely. The transverse kick seen by the electron from the beam ion with the impact parameter b is

$$\Delta p_\perp \approx m_e \Delta v_\perp \approx \frac{Z e^2}{2\pi\epsilon_0 \gamma_0 v b} = \frac{2 Z r_e c m_e}{\beta_0 b} \quad (12)$$

Assuming that the beam is infinite transversely with the particle density $\rho_i = N_i/(2\pi a^2 L)$ one can find the heating rate for infinite beam

$$W_h \approx \frac{1}{2m_e} \int_{b_{min}}^{b_{max}} 2\pi \Delta p_\perp^2(b) \beta c \rho_i(b) b \, db =$$
$$= E_0 \frac{4\pi c \rho_i Z^2 r_e^2}{\beta_0} \ln \Lambda \quad (13)$$

where r_e - electron classical radius, $\ln \Lambda = 10$ - Coulomb logarithm. Obtained heating rate saturates at the fixed level with the increasing beam energy. Here we neglect the relativistic effects that lead to an increase of heating rate with energy. If one neglects the electron space charge, then the saturated density of electrons is proportional to the production rate and inversely proportional to the heating rate. There are two main factors affecting the production rate namely residual gas pressure and beam energy. Reducing pressure below some threshold value will move saturated electron density below the instability threshold. In [13] it was also shown that the final neutralization degree does not depend on the ion. It only depends on the ion energy.

If the beam profile is realistic, then the heating rate as a function of electron coordinate is a complicated function. One has to average all the kicks that electrons see at different distances from the beam. This leads to the dependence of Coulomb logarithm on the coordinate. In our simulations we use a simplified model. We assume that the heating rate depends only on the local beam density. However, even with this simplifications it appears not easy to find analytical expressions for the electron life time and saturated density.

NUMERICAL MODEL

For the numerical simulations the Particle-in-Cell code with 2D beam-electron interaction was used. To simulate the residual gas ionization electron macroparticles were produced using the random number generator with the probability proportional to the local beam density.

All the macroelectrons were chosen to have equal charge. To speed up simulations after a certain threshold number of electrons is reduced and their charge is increased proportionally. Reflection from the wall and secondary emission were implemented similar to the ECLOUD code. However, at the wall no recalculation of the particle weight is done. Instead of that a number of new macroelectrons is produced proportional to the total secondary emission yield. The cloud itself is 2D and concentrated in the kick point.

Beam consists of rigid slices that can move transversely only as a whole. For the simulations of two-stream instability the only constraint is that this model does not allow longitudinal motion (tune spread) of beam particles. This removes the essential part of the Landau damping present in real beam-cloud interaction. To avoid this problem in [14] it was proposed to introduce a precalculated damping term. It was used to multiply transverse beam coordinates by it each turn. However, in this reference the damping appears to be constant for all the excited harmonics. For this reason we introduce separate damping terms for each oscillation harmonic assuming compensated chromaticity and negligible space charge tune shift:

$$\alpha_n = e^{-2\sqrt{2\pi}\eta\frac{dp}{p}n} \tag{14}$$

These damping terms agree with [12] and differ from [14]. The difference is most likely due to the different form factors of betatron frequency spread. In Eq. 14 a Gaussian momentum spread is assumed, whereas in [14] Keil-Zotter theory used where a parabolic frequency distribution is assumed. For future studies it is possible to calculate damping term for each harmonic taking into account other factors such as space charge tune shift and chromaticity.

In simulations each turn a Discrete Fourier transform is applied to the vector of beam transverse coordinates and momenta (x, y, x', y'). Signal on each j-th harmonic is then multiplied by its own damping term α_j and taking the inverse Fourier transform one gets a set of damped coordinates.

Heating rate was simulated using the stochastic term introduced in the electron equation of motion. Each time step electron experiencing the Coulomb heating receives the kick

$$\Delta p_{x,y} = \sqrt{m_e W_h(x, y)\Delta t} \cdot r_g \tag{15}$$

where r_g - is the random number having Gaussian distribution and $\sigma = 1$

SIMULATION RESULTS

First we have simulated the oscillation spectrum of the electron cloud produced by residual gas ionization. Fig. 1

Table 1: Simulation parameters

Parameter	Value
Circumference, [m]	1080
Ions	$U^{73+}, Ar^{18+}, Au^{25+}$
Vertical tune	17.29
Horizontal tune	20.309
Pipe radius, [cm]	5
Energy, [MeV]	400-1000
Momentum spread	$10^{-4} - 5 \cdot 10^{-4}$

shows that electron spectrum is very broad. Independent of beam species the relative form stays the same. One can see that the center of the trapping frequency is at 70% of the linear trapping frequency Eq. 6 To check in simulations
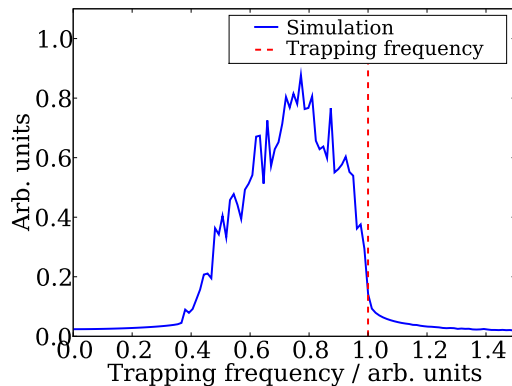

Figure 1: Spectrum of electrons produced by residual ionization in Gaussian coasting beam.

that ion beams limited by Eq. 4 have one and the same linear instability threshold we have assumed one and the same relatively fast neutralization rate $V_{neut} = 34.25s^{-1}$ for Ar^{18+}, U^{73+} and Au^{25+}. This way we can expect that the instability will start at the same time. Fig. 2 shows the behaviour of the vertical oscillation amplitude in time during the accumulation. Initial linear growth of the oscillation amplitude corresponding mainly to the real solutions of Eq. 1 is followed by a short exponential growth. It is interrupted because the cloud starts to grow and electrons move away from the linear resonance.

Substituting Eq. 6 to Eq. 9 and assuming that frequency spreads are constant the threshold neutralization degree should be inversely proportional to the beam intensity. To check this the scan over different intensities was made. Fig. 3 shows the neutralization factors at which the exponential instability growth is interrupted. It is seen that all 3 ions behave equivalently. Normalized to one and the same space charge tune shift their behaviour fits into one curve.

This way we have found and proved the equivalence of the heavy ion beams in absence of heating rate and electron space charge. As it was mentioned before Coulomb scattering can reduce the neutralization degree. In [13] it
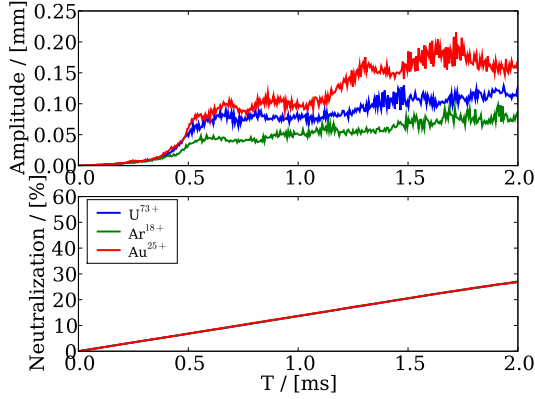
Figure 2: Maximum oscillation amplitude and neutralization degree. U^{73+}, Ar^{18+} and Au^{25+} beams at 400 MeV/u. Corresponding intensities are $6 \cdot 10^{10}$, $1.658 \cdot 10^{11}$ and $4.234 \cdot 10^{11}$. dp/p=10^{-4}
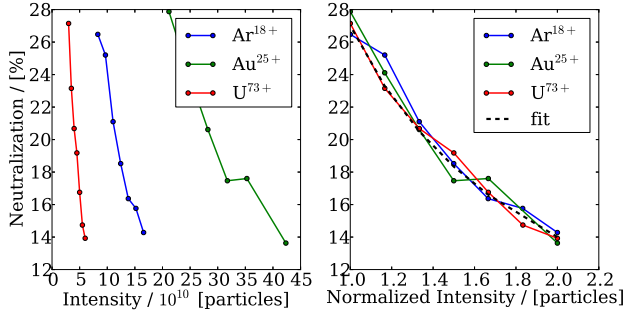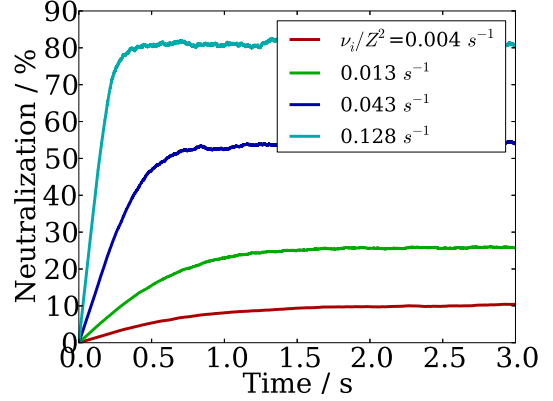

Figure 4: Neutralization degree reached for different production rates (pressures) taking into account electron space charge and the heating rate. The U^{28+} beam is fixed for these simulations. Energy is 1 GeV/u. The lowest production rate corresponds to $1.5 \cdot 10^{-11}$ Torr.
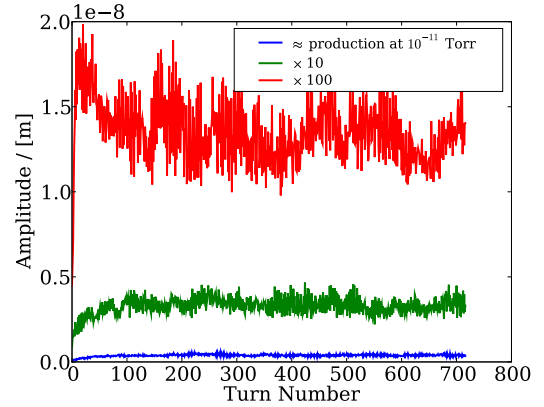

Figure 3: Neutralization degree at which linear instability starts as a function of beam intensity for 3 ion types. Relativistic β=0.7. Right graph shows the curves scaled to one spacecharge tune shift. Dashed line shows the fit following from Eq. 9

Figure 5: The amplitudes reached by the U^{73+} coasting beam assuming initial cloud distribution obtained in simulations for Fig. 4. N=$7 \cdot 10^{10}$, dp/p=10^{-4}

was shown that saturated neutralization degree due to the Coulomb heating is constant for different ion beams with similar parameters. Fig. 4 shows the saturated neutralization degree assuming electron space charge and heating rate for fixed beam position. One can see that the neutralization degree is strongly limited for the production rates corresponding to 10^{-11} Torr. However, for bigger residual gas density the neutralization degree becomes significant. Although, at such pressures other effects such as the beam loss due to charge exchange become important [15] and safe operation is impossible. Instability simulations for the given electron densities revealed oscillation with very tiny amplitudes (Fig. 5) which is not really dangerous for the slow extraction of intense heavy ion beams. Such a small amplitudes are probably due to the low local density of the cloud at the beam center. In case of continuous coasting beam no pinching happens.

STOPPING POWERS OF SHORT PROTON BUNCHES

This work was published in [5]. In CERN the synchronous phase shift due to the electron cloud was measured [16]. During beam storage the rf phase shift $\Delta\phi_s$ in a rf bucket is

$$\sin(\Delta\phi_s) = \frac{\Delta W_p}{qV_{rf}} \qquad (16)$$

where q - ion charge, V_{rf} - rf amplitude, ΔW_p - energy loss per particle per turn. In LHC the observed dependence of the rf phase shift on the bunch spacing indicates that electron clouds can be the source of the energy loss. In general the total energy loss of the bunch per unit length

$$S = \frac{dW_p}{ds} = -\int \rho_i(\vec{r})E_z(\vec{r})d^3r \approx -q\int \lambda(z)E_z(z)dz \qquad (17)$$

where ρ_i - bunch charge density, $E_z(z)$ - longitudinal electric field, $\lambda(z)$ - line density of the bunch. The energy loss per particle per turn is then

$$\Delta W_p = \frac{L}{N_i}\langle S\rangle \qquad (18)$$

For short bunches the stopping power can be obtained analytically if one assumes that the electrons see only a short impulse kick during the bunch passage

$$\Delta p_\perp(b) = \frac{1}{c}\int_{-\infty}^{\infty} F_\perp(b,s)ds, \quad F_\perp = -eE_\perp^i(b,s) \quad (19)$$

where $F_\perp$ is the transverse force seen by the electrons, $E_\perp^i(b,s)$ is the electric field of the bunch, b - transverse distance from the bunch center, s - longitudinal coordinate. In the field of the round K-V beam the total energy gain of the uniform electron distribution per unit length is

$$S = \frac{dW_e}{ds} = \frac{n_e}{2m_e}\int_0^{R_p} 2\pi\Delta p_\perp^2(b)bdb \approx \frac{Q_i^2 n_e r_e}{\epsilon_0}\ln(\frac{R_p}{a}) \quad (20)$$
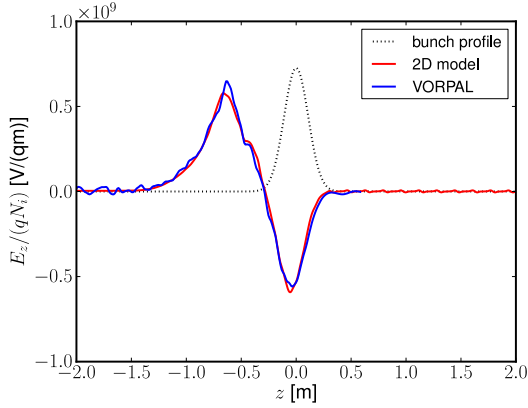
Electron cloud with growing density starts to behave more

Figure 6: Longitudinal electric eld obtained from the 2D ES and the 3D EM simulations for $n_e = 10^{12}m^{-3}$

like plasma. The stopping power in this case is connected with the energy transferred to the plasma waves. The equation of electron motion should be replaced with the plasma oscillator equation [17]:

$$\delta'' + \frac{\omega_{pe}^2}{c^2}\delta = \kappa^2(b,z) \qquad (21)$$

where δ - oscillator offset, $\kappa(b,z)$ - bunch force, ω_{pe} - plasma frequency. The resulting oscillator amplitude at $s = \infty$ is determined by

$$\hat{\delta}(b) = \frac{b}{\kappa_e}\int_{-\infty}^{\infty}\kappa(b,s)^2\cos(\kappa_e s) \qquad (22)$$

where $\kappa_e = \omega_{pe}/c$. The energy loss in this case is

$$\frac{dW_e}{ds} = \frac{1}{2}m_e n_e \omega_{pe}^2 \int_0^{R_p} 2\pi\hat{\delta}^2 bdb \qquad (23)$$

and the stopping power for $R_p \gg a$ is

$$S \approx \frac{Q_i^2\kappa_e^2}{4\pi\epsilon_0}\ln(\frac{R_p}{a})\exp(-\kappa_e^2\sigma_z^2) \qquad (24)$$

This is exactly the Eq. 20 multiplied by the exponential factor.

SIMULATION RESULTS

In simulations one can obtain the electron cloud wake fields and calculate the stopping power with the self-consistent space charge. Most of the results were obtained using simplified Particle-in-Cell code with 2D Poisson solver. To verify the results the full 3D electromagnetic simulations were performed using VORPAL. More details on the numerical models can be found in [5].

Fig. 6 and Fig. 7 show the comparison of the longitudinal wake fields in case of low and high (not negligible plasma frequency) electron cloud density. One can see that the agreement between two codes is very good for the given conditions. Fig. 8 shows the stopping power as a function
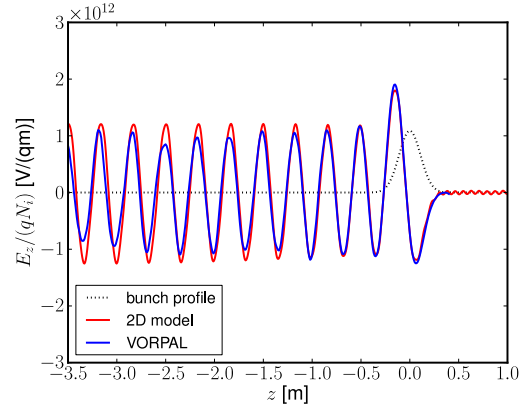

Figure 7: Longitudinal electric eld obtained from the 2D ES and the 3D EM simulations for $n_e = 10^{16}m^{-3}$

of bunch intensity. One can clearly see the deviation from Eq. 20. This happens because the kick approximation used to derive the equation is not valid for higher intensities. The dependence of the stopping power on the electron cloud density is shown in Fig. 9. One can see that at lower densities the agreement between simulations and theory is good. At higher density the analytical expression reproduces the simulation results only if the bunch length is assumed to be twice shorter.

As an additional step we have also performed simulations of the transverse wake fields using VORPAL and 2D ES code. We have simulated the fields induced by the bunches with an offset from the beam pipe axis and with a tilt relative to the pipe axis. The cloud density profiles and the bunch orientation are shown in Figs. 10 and 11. The wake fields are shown in Figs. 12 and 13. Fig. 12 shows the field induced by a bunch off-centered by 4 mm. Fig. 13 depicts the wake field of a bunch which having an angle between its axis and the beam pipe axis.
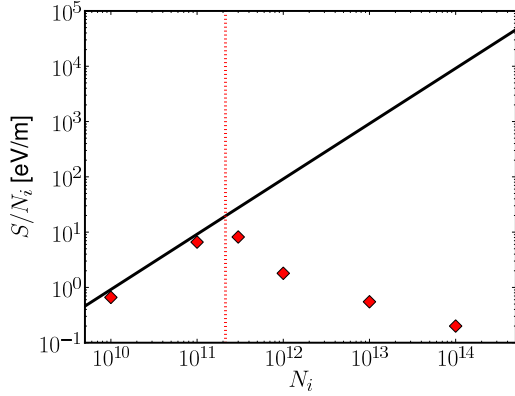
Figure 8: Stopping power as a function of the number of particles in the bunch. The analytic result is represented by the solid curve. The symbols represent the results obtained from the simulation. The red dashed line corresponds to $\kappa_0\sigma_z = 10$
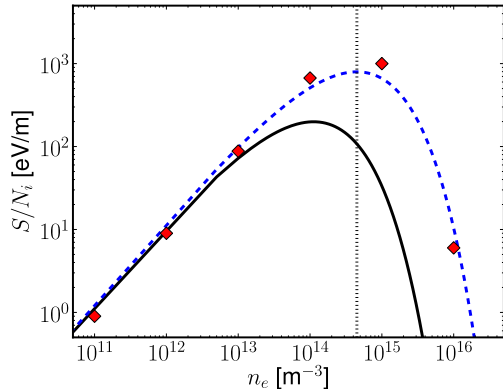

Figure 9: Stopping power as a function of the electron density. The analytic results obtained for $\sigma_z = 0.25m$ is represented by the solid curve. The symbols represent the results obtained from the simulations. The vertical, dotted line corresponds to $\kappa_e\sigma_z = 1$. The dashed blue curve corresponds to the analytical expression for $\sigma_z \rightarrow \sigma_z/2$.

CONCLUSIONS

Two separate problems were investigated in this contribution. The first one is the electron cloud accumulation and the instability in heavy-ion coasting beams in presence of residual gas ionization and Coulomb heating. The second one is the stopping power induced by the electron cloud pinched in the field of the short LHC like proton bunch.

It was found that beams having similar space charge tune shifts have equal neutralization instability thresholds in linear approximation. It means that if the coasting beams made of different species are stored long enough, all of them will reach the instability threshold under the bad vacuum conditions. However, if the storage time is small, then highly charged ions are in bigger danger because the neu-
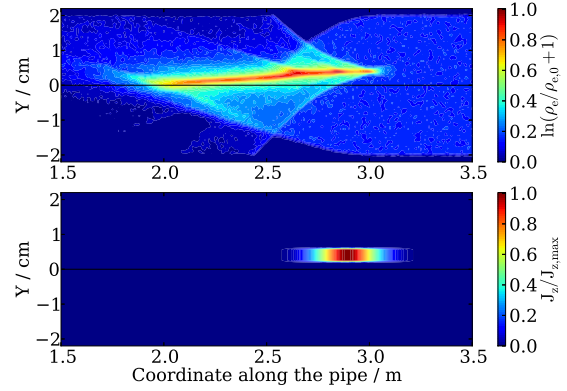

Figure 10: Electron cloud density profile and corresponding bunch orientation for the off-centered bunch. $\Delta x = 4mm$, N=10^{11}, σ_z=0.11 m.
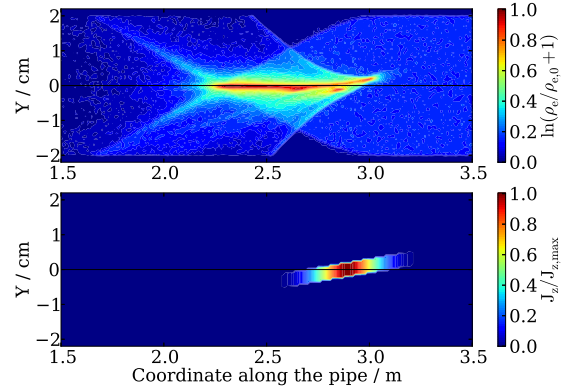

Figure 11: Electron cloud density profile and corresponding bunch orientation for the tilted bunch bunch. $\tan(\alpha) = 0.01$, N=10^{11}, σ_z=0.11 m.

tralization speed is $\propto Z$. For example, such ion as U^{73+} will reach the threshold 10 times faster than Ne^{7+}.

Modified rigid slice model including Landau damping was implemented to study the instability numerically. We have found out that for relatively high production rates at a certain electron density an exponential growth of the beam oscillation amplitude is observed. Similar behaviour was observed for three species when equal neutralization rates (ν_i/Z) were assumed. The scan over beam intensities revealed one and the same behaviour of the thresholds which is governed by Eq. 9. Thus the evidence of the equivalence of the heavy ion beams with intensities defined by a fixed space charge tune shift.

The electron cloud build-up simulations including Coulomb heating revealed that the total electron density can reach significant values above 10^{-10} Torr. At such pressures other effects such as charge exchange will significantly deteriorate the beam quality. For the design pressure
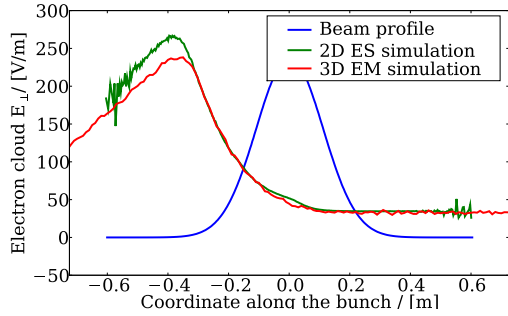
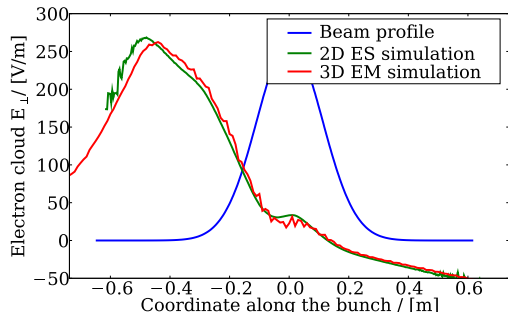Figure 12: Wake field induced by the off-centered bunch. $\Delta x = 4mm$, N=10^{11}, σ_z=0.11 m.

Figure 13: Wake field induced by the tilted bunch. $\tan(\alpha) = 0.01$, N=10^{11}, σ_z=0.11 m.

10^{-12} Torr the electron cloud density is close to 1% which is smaller than the simulated thresholds and no problems are expected. Generalizing the results it is found that for heavy-ion accelerators one can choose a residual gas pressure that completely removes the danger of the two-stream instability for any beam specie.

It was found out that the 2D ES model is sufficient to predict the stopping powers and wake fields induced in an electron cloud. We found that for sufficiently short bunches ($\kappa_0\sigma_z \leq 10$) the energy loss in a homogeneous cloud can be described very well by an analytic formula. For $\kappa_0\sigma_z \leq 10$ it was found that the stopping power scales according to $\propto Q_i^2$, which is equivalent to the effect of a longitudinal resistive impedance. For example if the cloud covers over 10% of the circumference and electron cloud density is 10^{12}m^{-3}, our analytical expression predicts an rf phase shift $\Delta\phi_s \approx 0.5$ deg in the LHC.

REFERENCES

[1] F. Zimmermann, Phys. Rev. ST Accel. Beams 7, 124801 (2004)

[2] R. Cimino, I. R. Collins, M. A. Furman, M. Pivi, F. Ruggiero, G. Rumolo, and F. Zimmermann, Phys. Rev. Lett. 93, 014801

[3] M. A. Furman and M. T. F. Pivi, Phys. Rev. ST Accel. Beams 5, 124404

[4] G. Rumolo, O. Boine-Frankenheim, GSI-Acc-Note-2003-10-00

[5] O. Boine-Frankenheim, E. Gjonaj, F. Petrov, F. Yaman, T. Weiland, and G. Rumolo , Phys. Rev. ST Accel. Beams 15, 054402

[6] G.I. Budker, Atomnaya energiya, No. 5, 9 (1956)

[7] K.Y. Ng, Physics of Intensity Dependent Beam Instabilities, 2006

[8] W. Schnell and B. Zotter, CERN Report ISR-GS-RF/76-26 (1976)

[9] I. Kaganovich, E. Startsev, R.C. Davidson, 2006 New J. Phys. 8 278

[10] F. Baconnier, A. Poncet and R.F. Tavarez, CAS Proceedings, CERN 9401, Geneve, p. 525, 1994

[11] FAIR Baseline Technical Report, March 2006

[12] A. Hofmann, "Landau Damping", CERN, Geneva, Switzerlan

[13] P.Zenkevich, N. Mustafin and O. Boine-Frankenheim, Adiabatic Theory of Electron Oscillations and Its Application to SIS100/SIS200, Proceedings of Ecloud-2002

[14] K. Ohmi, T. Toyama and G. Rumolo, Proceedings of ECLOUD'04, p.3083-3085

[15] P. Puppel, P. Spiller and U. Ratzinger, DYNAMIC VACUUM STABILITY IN SIS100, Proceedings of IPAC2011, San Sebastin, Spain

[16] J. Esteban-Müller and E. Shaposhnikova, This Workshop Proceedings

[17] P. Mulser, K. Niu, and R. Arnold, Nucl. Instrum. Methods Phys. Res., Sect. A 278, 89 (1989)